Effect of sophoridine on Ca^{2+} induced Ca^{2+} release during heart failure

S.-T. HU [1*], Y.-F. SHEN[2*], J.-M. GONG[3], Y.-J. YANG[2]

[1]Department of Physiology, Ningxia Medical University, Yinchuan, Ningxia, People's Republic of China, [2]Department of Biophysics, Second Military Medical University, Shanghai, People's Republic of China, [3]Department of Vasculocardiology, Second Affiliated Hospital of Ningxia Medical University, Yinchuan Ningxia, People's Republic of China

Summary

Sophoridine is a type of alkaloid extract derived from the Chinese herb Sophora flavescens Ait (kushen) and possess a variety of pharmacological effects including anti-inflammation, anti-anaphylaxis, anti-cancer, anti-arrhythmic and so on. However, the effect of sophoridine on heart failure has not been known yet. In this study, the effect of sophoridine on heart failure was investigated using Sprague–Dawley（SD）rat model of chronic heart failure. Morphological results showed that in medium and high dose group, myofilaments were arranged orderly and closely, intermyofibrillar lysis disappeared and mitochondria contained tightly packed cristae compared with heart failure group. We investigated the Ca^{2+} induced Ca^{2+} transients and assessed the expression of ryanodine receptor (RyR2) and L-type Ca^{2+} channel (dihydropyridine receptor, DHPR). We found that the cytosolic Ca^{2+} transients were markedly increased in amplitude in medium ($\Delta F/F_0$=43.33±1.92) and high dose groups ($\Delta F/F_0$= 47.21±1.25) compared with heart failure group ($\Delta F/F_0$=16.7±1.29, P<0.01), Moreover, we demonstrated that the expression of cardiac DHPR was significantly increased in medium- and high dose-group compared with heart failure rats. Our results suggest that sophoridine could improve heart failure by ameliorating cardiac Ca^{2+} induced Ca^{2+} transients, and that this amelioration is associated with upregulation of DHPR.

Key words

Heart failure • Sophoridine • Ca^{2+} induced Ca^{2+} release • L-type Ca^{2+} channel

Corresponding author

Yong-Ji Yang, Department of Biophysics, Second Military Medical University, Shanghai, 200433, People's Republic of China. Fax: +86-21-81870923. E-mail: yjyang22@163.com

***Contributed equally**

Introduction

Heart failure (HF) is a complex disorder characterized by contractile dysfunction and activation of neurohumoral factors (Majeed *et al*. 2005). It remains a major cause of death and disability all over the world in recent years. Among a variety of factors, abnormal regulation of Ca^{2+} by L-type Ca^{2+} channel (LTCC) and sarcoplasmic reticulum (SR) is underlying mechanism for muscle dysfunctions in HF (Middlekauff *et al*. 2012). Western drugs have been used for the treatment of HF and have proven to be effective. However, the efficacy of the most currently used western drugs for long-term prevention of heart failure in high risk patients has always been limited by their adverse reaction (Moe *et al*. 2012). Accordingly, the search for new types of cardioprotective drugs is an important area. In many cases of cardiac disease, altered Ca^{2+} cycling precedes the observed depression of mechanical performance, suggesting that an amelioration of the disorder of Ca^{2+} cycling will be the effective therapeutic strategy against heart failure (Gorski *et al*. 2015, Choi *et al*. 2014).

Sophoridine is a type of alkaloid extract derived from the Chinese herb Sophora flavescens Ait (kushen). The structure of sophoridine is clear as shown in Fig.1. In both basic and clinical studies, it has been confirmed to possess a variety of pharmacological effects including anti-inflammation, anti-anaphylaxis, anti-oxidant, anti-cancer, anti-arrhythmic and so on (Liu *et al*. 2015, Wang *et al*. 2014, Ma *et al*. 2013, Zhao *et al*. 2010). A study on mechanisms showed that sophoridine could inhibit scavenge hydroxy radicals and influence ion channels of cardiomyocytes.

Therefore, we speculate that sophoridine may be able to exert a protective effect on the

cardiovascular system. To test this hypothesis, the present experiments were designed to assess the cardioprotective effect of sophoridine using a rat model of chronic heart failure as well as to further identify its underlying mechanisms.

Materials and Methods

Surgical procedure and animal models

Male Sprague–Dawley rats weighing (180~200g) were housed in an accredited laboratory animal facility and all procedures were performed in accordance with the protocols approved by the Institutional Animal Care and Use Committee of the Ningxia Medical University. The animals were randomly divided into 5 groups (n=10 for each group): myocardial infarction (MI) group, high-dose group (rats with MI and 10mg/kg sophoridine treatment), medium-dose group (rats with MI and 5mg/kg sophoridine treatment), low-dose group (rats with MI and 2.5mg/kg sophoridine treatment) and sham operated group. The animals were randomized to receive either myocardial infarction (MI) (Tanonaka *et al*. 2010) or a sham procedure.

Rats were deeply anesthetized with intraperitoneal injection of 10% chloral hydrate (3ml/kg), Following intubation and placement on a respirator, a left lateral thoracotomy was performed in the 3nd and 4th intercostal space, and a ligature was placed around the left anterior descending coronary artery 2mm below its origin. Ischemia was verified by visual inspection, the chest was closed, and the rat was extubated and returned to its cage. Sham-operated animal under went the same procedure without ligation of the left anterior descending coronary artery.

Drug administration

Sophoridine injection was diluted in saline to prepare concentrations of 2.5mg/ml. For high-, medium- and low-dose group, sophoridine at doses of 10, 5 and 2.5mg/kg. They were administered respectively by intraperitoneal injection, immediately after myocardial infarction and once daily on the following 28 days. In the case of the MI and sham operated group, equal volume saline was administered in the same manner.

Assessment of heart function

28 days after MI, the rats were anesthetized with 10% chloral hydrate and placed on a pad. A micromanometer catheter was introduced into the right carotid artery and advanced across the aortic valve into the left ventricular cavity to record left ventricular pressures. Left ventricular end-diastolic pressure (LVEDP) and the maximum rates of contraction (d*p*/d*t*max) and relaxation (d*p*/d*t*min) were derived from the left ventricular pressure pulse (van Rooij *et al*. 2004). Each hemodynamic evaluation was completed within 15-25 minutes. At the termination of the functional study, the heart was removed and its weight was obtained.

Cell dissociation and patch-clamp study

Single cardiomyocytes (left ventricle cell) of the rat heart were isolated by an enzymatic dissociation method (Ohmoto-Sekine *et al*. 1999). The heart was removed from the open chest of rats anaesthetized with 10% chloral hydrate and mounted on a modified Langendorff perfusion system for retrograde perfusion with Ca^{2+}-free Tyrode's solution; then the heart was perfused with the solution containing collagenase Ⅱ and bovine serum albumin for about 10 minute. After digestion, ventricular myocardium tissue was cut into small pieces in the modified Kraft-Bruhe (KB) solution (Nakaya 1993) and gently shaken to dissociate cells. All experiments were conducted at room temperature (20-22℃).

Whole-cell patch clamp recordings of transmembrane ionic currents were performed with an EPC10 amplifier (HEKA Instruments, Germany). Cardiomyocytes were placed in a perfusion chamber. Patch electrodes were fabricated from borosilicate glass with a Micropipette Puller. Its resistance was 2-4 MΩ when the electrode was filled with the pipette solution. The potential of the electrode was adjusted to zero current between the pipette solution and the bath solution immediately before seal formation. After obtaining a gigaseal, a suction pulse was applied to establish the whole-cell mode. Command pulses were delivered and data were acquired with a patch-clamp amplifier controlled by the PULSE software connected to a compute. In the end, data analysis was performed.

Laser scanning confocal microscope analysis

Intracellular Ca^{2+} imaging was performed using Leica TCS SP2 confocal microscope (Leica, Germany) in line-scan mode. Cytosolic Ca^{2+} measurements was performed using Fluo-3/AM Ca^{2+} indicators. When measured, Fluo-3/AM was excited by the 488 nm line of an argon-ion laser, and the fluorescence was acquired at wavelengths 500-560 nm. Patch-clamp and confocal microscope synchronous recording system software was used to record transmembrane Ca^{2+} currents ($I_{Ca\cdot L}$) and intracellular Ca^{2+} sparks simultaneously.

For quantitative studies, the temporal dynamics in fluorescence were expressed as $\Delta F/F_0 = (F–F_0)/F_0$, where F represents fluorescence at time t and F_0 stands for baseline fluorescence.

Real-time quantitative reverse transcription polymerase chain reaction (RT-PCR) analysis

The mRNA levels of RyR2 and LTCC（DHPR）were measured using real-time quantitative RT-PCR. The total RNA was extracted from the homogenate using Trizol reagent and reversely transcribed to cDNA by using reverse transcriptase according to previous publications and the manufacturer's instructions (Qi *et al*. 2006). Reverse transcription was performed in a 30μl reaction mixture, at 40℃ for 60min and 70℃ for 10min. The total volume of the PCR reaction was 50μl: 1μl cDNA, 2mmol/L $MgCl_2$, 20mmol/L each dNTP, 0.2nmol/L each primer, 2u DNA Taqpolymerase and the accompanied buffer. Real-time PCR was carried out on Real-time Quantitative PCR System (FTC2000，Canada) for the detection of PCR products. The temperature profile was as follows: 93℃ for 4min, followed by 40 cycles of 93℃ for 20s, 60℃ for 30s, and 72℃ for 45s. At the end of each extension step, the fluorescence intensity was read on the Light cycler. Melting curve analyses were created following the final PCR cycle to confirm the presence of a single PCR product. In the experiment, GAPDH mRNA was used as the internal control for each sample since it was consistently expressed in all the cells. The specific primers for RyR2 were: sense,5'-TAACCTACCAGGCCGTGGAT-3'antisense,5'-GCTGCGATCTGGATAAGTTCAA-3'; forDHPR:sense,5'-CATCTTTGGATCCTTTTTCGTTCT-3'antisense,5'-TCCTCGAGCTTTGGCTTTCTC-3'andforGAPDH:sense,5'-TGGAGTCTACTGGCGTCTT-3'antisense,5'-TGTCATATTTCTCGTGGTTCA-3', respectively.

Immunoblotting

RyRs protein was immunoprecipitated from 500μg (total protein) samples by overnight incubation with mouse anti-RyR (Jayaraman *et al*. 1992), followed by incubation with protein G PLUS-Agarose at 4℃ for an additional 1h, and then the beads were washed three times with ice-cold buffer, each time for 10 min. The proteins bound to the Sepharose beads were then solubilized by the addition of Laemmli's sample buffer plus 5% (v/v) β-mercaptoethanol and boiled for 5 min. The samples were then separated on sodium dodecyl sulphate gel electrophoresis (SDS/PAGE) (6% separation gel for RyR2). The SDS/PAGE-resolved proteins were transferred to nitrocellulose membranes at 30 mA for 16.5 h at 4°C. The nitrocellulose membranes containing the transferred proteins were blocked for 1h with PBS containing 0.5% Tween 20 and 5% (w/v) skimmed milk. The blocked membranes were then incubated with antibody (1:1,000) for 1h and washed three times for 5 min in PBS containing 0.5% Tween-20. The membrane was then incubated with the appropriate horseradish peroxidase-conjugated secondary antibody (1:5,000) for 1h. After washing three times for 5 min each in PBS containing 0.5% Tween 20, these proteins were detected by enhanced chemiluminescence (ECL). Band densities were quantified by using LabWorks4.6 software (PerkinElmer). The level of DHPR protein is also determined by immunoblot analysis. Cell lysate proteins is subjected to SDS 8% and 6% PAGE, blotted onto nitrocellulose membranes, and probed with anti-DHPRα1.

Drugs and solutions

Sophoridine injection was purchased from Tong-hua Fangda Pharmaceutical Co. Ltd. (China); Fluo-3/AM was purchased from Biotium; TRIzol Reagent was purchased from Invitrogen Life Technologies (USA), RyR antibody and DHPRα1 antibody were purchased from Abcam and collagenase type Ⅱ was purchased from Worthington (USA). All other reagents were purchased from Sigma (USA). The composition of the Ca^{2+}-free Tyrode's solution was (in mM) NaCl 135, KCl 5.4, $MgCl_2$ 1.0, NaH_2PO_4 0.33, glucose 5.0, and HEPES 5.0 (pH 7.3). The composition of the digestion solution was Ca^{2+}-free Tyrode's solution 25ml, collagenase type Ⅱ 15mg, BSA 50mg,

and 72mmol/L $CaCl_2$ 20μl. The composition of the modified Kraft-Bruhe (KB) solution was (in mM) KOH 80, L-glutamic acid 50, KCl 30, taurine 20, KH_2PO_4 30, $MgCl_2$ 3, glucose 10, EGTA 0.5, and HEPES 10 (pH 7.3). The external solution contained (in mM) NaCl 133.5, CsCl 4.0, $CaCl_2$ 1.8, $MgCl_2$ 1.2, HEPES 10, and glucose 11.1 (pH 7.3). Patch pipettes were filled with a solution that contained (in mM) CsCl 120, TEA-Cl 10, Na_2ATP 5, $MgCl_2$ 6.5, Tris GTP 0.1, and HEPES 10 (pH 7.2).

Statistical analysis

Data were expressed as mean ± S.E. for all the experiments. Statistical analysis were made with ANOVA and followed by Student–Newman–Keuls test for individual comparisons of means. *P*-values of <0.05 were considered significant.

Results

Characterization of cardiac function

Hemodynamic responses were assessed in different groups (Table 1). The maximal change in systolic pressure over time (dp/dt_{max}) was significantly increased by sophoridine at a dose of 5mg/kg (3,891.12±238.81mmHg/s, *n*=10) and 10 mg/kg (3,825.72±250.08mmHg/s, *n*=10) versus HF group (2,329.64±227.27mmHg/s, *n*=10, *P*<0.01). At a dose of 2.5 mg/kg, sophoridine increased the dp/dt_{max}, but a significance level was not reached. The left ventricular end-diastolic pressure(LVEDP) was significantly decreased by sophoridine at a dose of 5mg/kg (5.8±1.2mmHg, *n*=10) and 10 mg/kg (5.6±1.3mmHg, *n*=10) versus HF group (8.7±1.5mmHg, *n*=10, *P*<0.01). Furthermore, there was a significant decrease in heart weight (HW) divided by body weight (BW) in medium-dose (3.01±0.23, *n*=10) and high-dose group (3.05±0.25, *n*=10) compared with HF rats (4.56±0.17, *n*=10, *P*<0.05), respectively.

Measurement of $I_{Ca\cdot L}$ and ACT

Depolarization-induced $I_{Ca\cdot L}$ and spatially resolved intracellular Ca^{2+} transients (action potential-induced Ca^{2+} transients, ACT) were measured in cardiomyocytes dialyzed with Fluo-3/AM. The representative traces of $I_{Ca\cdot L}$ and confocal line-scan images along with the spatial

average of Ca^{2+} transients recorded during a depolarizing step from −40 to +10 mV in cardiac myocytes from different groups are shown in Figure 2. The amplitude of $I_{Ca\cdot L}$ was increased in medium- (4.47±0.52, n=20 cells from ten medium dose sophoridine -treated hearts) and high-dose group (5.01±0.49, n=20 cells from ten high dose sophoridine-treated hearts) compared with HF group (1.23±0.09, n=20 cells from ten HF hearts, P<0.01) (Figure 2). Moreover the amplitude of Ca^{2+} transients was also increased in medium- and high-dose group (Figure 3). There was a significant increase in spatial averages ($\Delta F/F_0$) of $I_{Ca\cdot L}$-induced Ca^{2+} transients in medium (43.33±1.92, n=12 cells from six medium dose sophoridine-treated hearts) and high dose group (47.21±1.25, n=12 cells from six high dose sophoridine-treated hearts) compared with HF group (16.7±1.29, n=12 cells from six HF hearts, P<0.01) (Figure 4).

Observation under transmission electron microscopy

The ultrastructure of myocardial cells in left ventricle of a SD rat was studied under transmission electron microscopy (TEM). In control group (Figure 5A), the myocardial cell appeared normal with intact sarcomeres, mitochondria contain tightly packed cristae. Numerous glycogen granules were present. In HF group (Figure 5B), some parts of the myocardial cell showed intermyofibrillar lysis and vesicles of varying size. Mitochondria were swollen, and mitochondrial cristae were separated. In group treated by low-dose of sophoridine (Figure 5C), intermyofibrillar lysis slightly restored, but a few mitochondria were still swollen, and mitochondrial cristae were separated. In group treated by medium-dose of sophoridine (Figure 5D), intermyofibrillar lysis disappeared, myofilaments were orderly, closely, and evenly arranged, and mitochondria contained tightly packed cristae. The ultrastructure of myocardial cells, treated by high-dose of sophoridine (Figure 5E), was similar with that treated by medium dose of sophoridine, and electron density of some mitochondria increased.

Effects of sophoridine on the mRNA expressions of Ca^{2+} handling genes

Real time quantitative RT-PCR was performed to determine the relative mRNA expression pattern of RyR2 and DHPR. We found that the mRNA expression of RyR2 was not

altered in medium- and high-dose group compared with HF group (n=8, P>0.05). The mRNA expression of DHPR was significantly enhanced in medium- and high-dose group compared with HF group (n=8, P<0.01). (Figure 6).

Effects of sophoridine on expressions of Ca^{2+} handling proteins

Immunoblot analyses were performed to determine the contents of the major Ca^{2+} handling proteins RyR2 and DHPR in five groups. Compared with channel complexes from HF rat, the expression of RyR2 in low-, medium- and high-dose group failed to alter (n=6, P>0.05), whereas DHPR content was significantly enhanced in medium- and high-dose group (n=6, P<0.01). (Figure 7,8)

Discussion

Heart failure (HF) and sudden cardiac death are escalating major health problems worldwide. Despite the availability of several treatment modalities, heart failure patients still have high morbidity and mortality (Bhatt *et al.* 2015). A considerable amount of evidence in the literature indicates the important role of Ca^{2+} in the pathogenesis of heart failure and sudden cardiac death. Defective intracellular Ca^{2+} homeostasis has been consistently reported in heart failure (Kalyanasundaram *et al.* 2013, Rozentryt *et al.* 2015).

In excitation–contraction coupling (ECC) of cardiomyocytes, the depolarization signal of the cell membrane opens the L-type Ca^{2+} channel (LTCC) / dihydropyridine receptor (DHPR), and the resulting relatively small Ca^{2+} influx then triggers a thousand fold greater Ca^{2+} release from sarcoplasmic reticulum (SR) via ryanodine receptor (RyR2). Ca^{2+} induced Ca^{2+} release (CICR) is an amplification mechanism of Ca^{2+} signals, by which local Ca^{2+} increases at the cytoplasmic side trigger Ca^{2+} release from the SR to generate global Ca^{2+} signaling for contraction in cardiomyocytes. In the relaxation phase, cytoplasmic Ca^{2+} is pumped into the SR by Ca^{2+}-ATPase (SERCA2a) or discharged to the extracellular fluid by type 1 Na^{+}-Ca^{2+} exchanger (NCX1) (Hasenfuss *et al.* 1994, Hasenfuss *et al.* 1999). An alteration in ECC is one of the possible factors in the pathogenesis of heart failure. Impaired calcium transient is a key factor for an alteration of ECC, leading to

contractile dysfunction and the development of ventricular arrhythmias. Characteristics of Ca^{2+} cycling in heart failure include a decreased amplitude of the Ca^{2+} transient, a slow rate of diastolic Ca^{2+} decay, and an increased diastolic Ca^{2+}.

Sophoridine has been demonstrated to have a variety of pharmacological actions. Accumulating evidence indicates that matrine may exert a protective effect on the cardiovascular system. Yu J (Yu *et al*. 2014) have showed that matrine improved the function of failing heart in rats via inhibiting apoptosis and blocking beta3 adrenoreceptor/endothelial nitric oxide synthase pathway. In the present study, we demonstrate that sophoridine was a potent cardioprotective agent in ischemia-induced heart failure. Our data suggest that sophoridine may improve cardiac muscle function by reversing a maladaptive defect in intracellular Ca^{2+} signaling in heart failure. We found that administration of 5mg/kg sophoridine was sufficient to provide significant cardioprotection against heart injury induced by myocardial infarction. We supported this finding by both functional (electrophysiological) and morphological data: an increased Ca^{2+} transients (action potential-induced Ca^{2+} transients), which is considered to be critical hallmarks of amelioration of heart failure. And a series of morphological amelioration was observed under electron microscopy. In group with treated by medium- and high-dose of sophoridine, intermyofibrillar lysis disappeared, myofilaments were orderly, closely, and evenly arranged, and mitochondria contain tightly packed cristae.

At a dose of 2.5mg/kg, sophoridine had no significant protective effect, so the cardioprotective effect of sophoridine was dose dependant. The minimum effective dose of sophoridine may be between 2.5 to 5mg/kg, and needs further study.

Depolarization of the plasma membrane by an incoming action potential activates voltage-gated L-type Ca^{2+} channels in plasma membrane invaginations called T-tubules. In the heart, LTCC (DHPR) activation results in a plasma membrane Ca^{2+} influx current, which triggers RyR2 activation and SR Ca^{2+} release, referred to as CICR. The ability of the trigger (the Ca^{2+} influx through $I_{Ca\cdot L}$-channels) to induce much higher release of Ca^{2+} from the SR has been termed E-C

coupling gain. In many cases of HF, the E-C coupling gain seems to be reduced by a functional defect in LTCC, an increase in the space between LTCC and RyR2, a decrease in SR Ca^{2+} and/or an abnormality in the channel-gating property of RyR2. Not only the amount of Ca^{2+} released for a given Ca^{2+} release trigger but also the rate of Ca^{2+} release may be important for the contractility of the myofilaments. The present study shows that the expression of DHPR seems to be increased in medium- and high- dose group compared with HF group, which leads to the increased amplitude of $I_{Ca\cdot L}$ and the increased Ca^{2+} release (action potential-induced Ca^{2+} transients).

In China, pure sophoridine injection has been available in hospital for treatment of tumor for many years. However, it has not been used for heart failure in clinic. Since our results indicate that sophoridine prevents rat from heart failure, we hope that sophoridine can be used to treat heart failure although further research should be carried out on more animal experiments before clinical trials.

In this paper, we found that sophoridine had a beneficial effect on heart failure in rat for the first time. Although details of the mechanism of sophoridine remain to be unraveled, the present results suggest that sophoridine improves cardiac function by ameliorating CICR, and that this amelioration is associated with upregulation of DHPR. Therefore, we suggest that sophoridine maybe a novel, effective therapeutic drug for the treatment of hear failure.

Conflict of Interest

There is no conflict of interest.

Acknowledgements

This work was supported by The National Natural Sciences Fund Project of China (NSFC, 81260051),. We thank Pro. Xu-Ting Ye for his technical assistance and Yong-Zhong Zhou for providing valuable suggestions.

References

MAJEED A, WILLIAMS J, DE LUSIGNAN S, CHAN T: Management of heart failure in primary

care after implementation of the National Service Framework for Coronary Heart Disease: a cross-sectional study. *Public Health* **119**: 105-111, 2005.

MIDDLEKAUFF HR, VIGNA C, VERITY MA: Abnormalities of calcium handling proteins in skeletal muscle mirror those of the heart in humans with heart failure: a shared mechanism? *J Card Fail* **18**: 724-33, 2012.

MOE G.W, EZEKOWITZ JA, O'MEARA E.: The 2014 Canadian Cardiovascular Society Heart Failure Management Guidelines Focus Update: anemia, biomarkers, and recent therapeutic trial implications. *Can J Cardiol* **31**: 3-16, 2012.

GORSKI PA, CEHOLSKI DK, HAJJAR, RJ:ALTERED myocardial calcium cycling and energetics in heart failure-a rational approach for disease treatment. *Cell Metab* **21**: 183-94, 2015.

CHOI E, CHA MJ, HWANG KC: Roles of Calcium Regulating MicroRNAs in Cardiac Ischemia-Reperfusion Injury. *Cells* **3**: 899-913, 2014.

LIU ZW, WANG JK, QIU C: Matrine pretreatment improves cardiac function in rats with diabetic cardiomyopathy via suppressing ROS/TLR-4 signaling pathway. *Acta Pharmacol Sin* 36: 323-33, 2015.

WANG CY, BAI XY, WANG CH: Traditional Chinese medicine: a treasured natural resource of anticancer drug research and development. *Am J Chin Med* **42**: 543-59, 2014.

MA ZJ, LI Q, WANG JB: Combining Oxymatrine or Matrine with Lamivudine Increased Its Antireplication Effect against the Hepatitis B Virus In Vitro. *Evid Based Complement Alternat Med* 186573, 2013.

ZHAO WC, SONG LJ, DENG HZ: Effect of sophoridine on dextran sulfate sodium-induced colitis in C57BL/6 mice. *J Asian Nat Prod Res* **12**: 925-33, 2010.

TANONAKA K, FURUHAMA KI, YOSHIDA H: Protective effect of heat shock protein 72 on contractile function in the perfused failing heart. *Am J Physiol Heart Circ Physiol* **281**: H215-H222, 2010.

VAN ROOIJ E, DOEVENDANS PA, CRIJNS HJ: MCIP1 overexpression suppresses left ventricular remodeling and sustains cardiac function after myocardial infarction. *Circ Res* **94**: e18-26, 2004.

OHMOTO-SEKINE Y, UEMURA H, TAMAGAWA M: Inhibitory effects of aprindine on the delayed rectifier K^+ current and the muscarinic acetylcholine receptor-operated K^+ current in guinea-pig atrial cells. *Br J Pharmacol* **126**: 751-761, 1999.

NAKAYA H, TOHSE N, TAKEDA Y: Effects of MS-551, a new class antiarrhythmic drug, on action potential and membrane currents in rabbit ventricular myocytes. *Br J Pharmacol* **109**: 157-163, 1993.

QI M XIA HJ，DAI DZ, DAI Y: A novel endothelin receptor antagonist CPU0213 improves diabetic cardiac insufficiency attributed to up-regulation of the expression of FKBPl2.6, SERCA2a，and PLB in rats. *J Cardiovascular Pharmacology* **47**:729-735, 2006.

JAYARAMAN T, BRILLANTES AM., TIMERMAN AP: FK506 binding protein associated with the calcium release channel (ryanodine receptor). *J Biol Chem* **267**: 9474-9477, 1992.

BHATT, H, SAFFORD, M, GLASSER, S: Coronary Heart Disease Risk Factors and Outcomes in the Twenty-First Century: Findings from the REasons for Geographic and Racial Differences in Stroke (REGARDS) Study. *Curr Hypertens Rep* **17**: 541, 2015.

KALYANASUNDARAM A, LACOMBE VA, BELEVYCH AE: Up-regulation of sarcoplasmic reticulum Ca^{2+} uptake leads to cardiac hypertrophy, contractile dysfunction and early mortality in mice deficient in CASQ2. *Cardiovasc Res* **98**: 297-306, 2013.

ROZENTRYT, P, NIEDZIELA JT, HUDZIK B: Abnormal serum calcium levels are associated with clinical response to maximization of heart failure therapy. *Pol Arch Med Wewn* **125**: 54-64, 2015.

HASENFUSS G, REINECKE H, STUDER R: Relation between myocardial function and expression of sarcoplasmic reticulum Ca^{2+}-ATPase in failing and nonfailing human myocardium. *Circ Res* **75**: 434-442, 1994.

HASENFUSS G, SCHILLINGER W, LEHNART SE: Relationship between Na^{+}-Ca^{2+} exchanger protein levels and diastolic function of failing human myocardium. *Circulation* **99**: 641-648, 1999.

YU J, YANG S, WANG X: Matrine improved the function of heart failure in rats via inhibiting apoptosis and blocking beta3adrenoreceptor/endothelial nitric oxide synthase pathway. *Mol Med Rep* **10**: 3199-204, 2014.

Table

Table 1 Assessment of cardiac function in different groups

	sham	HF	Low dose	Medium dose	High dose
Number	**10**	**10**	**10**	**10**	**10**
BW (g)	**221.5±15.1**	**219.2±13.3**	**231.7±22.9**	**226.5±15.4**	**231.8±18.2**
HW/BW (mg/g)	**2.35±0.22**	**4.56±0.17****	**4.34±0.41**	**3.01±0.23$^{\Delta}$**	**3.05±0.25$^{\Delta}$**
HR (beats/min)	**431±17**	**443±22**	**428±24**	**438±21**	**426±16**
LVEDP (mmHg)	**4.9±1.2**	**8.7±1.5****	**8.9±1.8**	**5.8±1.2$^{\Delta\Delta}$**	**5.6±1.3$^{\Delta\Delta}$**
dp/dt_{max} (mmHg/s)	**4,337.19±212. 35**	**2,329.64±227.27****	**2,511.52±219.23**	**3,891.12±238.81$^{\Delta\Delta}$**	**3,825.72±250.08$^{\Delta\Delta}$**
dp/dt_{min} (mmHg/s)	**−2,912.57±255.57**	**−1,498.51 ±162.42****	**−1,574.25 ±160.39**	**−2,588.06 ±144.71$^{\Delta\Delta}$**	**−2,606.36±205.87$^{\Delta\Delta}$**

MI myocardial infarction, *BW* Body weight, *HW* heart weight, *HR* heart rate, *LVEDP* left ventricular end-diastolic pressure, dp/dt_{max} maximum change in systolic pressure over time, dp/dt_{min} maximum change in the rate of relaxation over time. Data are presented as mean ± S.E. 1mmHg = 0.133kPa **$P < 0.01$ HF versus sham, *$P < 0.05$ HF versus sham, $^{\Delta\Delta}P < 0.01$ Medium dose, High dose versus HF, $^{\Delta}P < 0.05$ Medium dose, High dose versus HF.

Figures

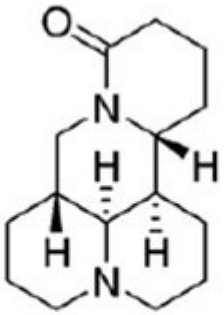

Figure 1. Chemical structure of sophoridine

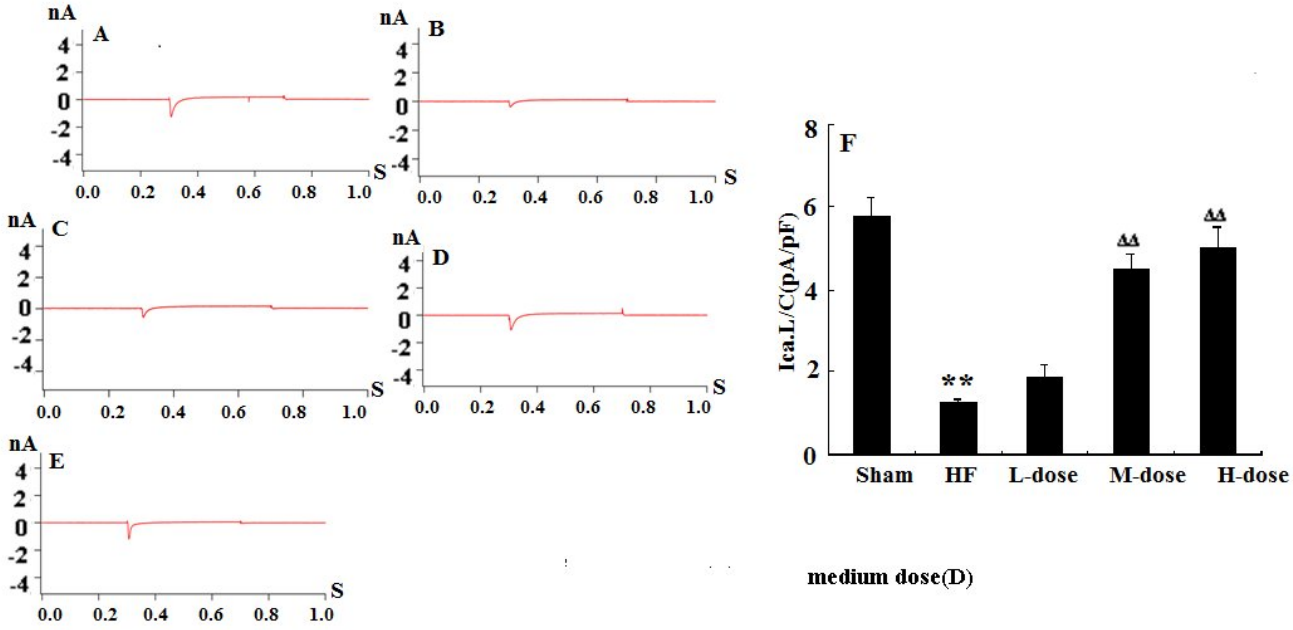

Figure 2. Recordings of $I_{Ca\cdot L}$ in sham operated group(A), HF (B), low dose(C),medium dose(D)and high dose(E) group. The average current/capacitance (pA/pF) were 5.78±0.44 in sham operated, 1.23±0.09 in HF, 1.87±0.31 in low dose, 4.47±0.52 in medium dose and 5.01±0.49 in high dose group(F). (n = 20, **P<0.01 versus sham group; $^{\Delta\Delta}P$<0.01 versus HF), The current was obtained in response to 400ms depolarizing step to +10mV after a prepulse to -40mV for 300ms inactivated sodium current from a -40mV holding potential.

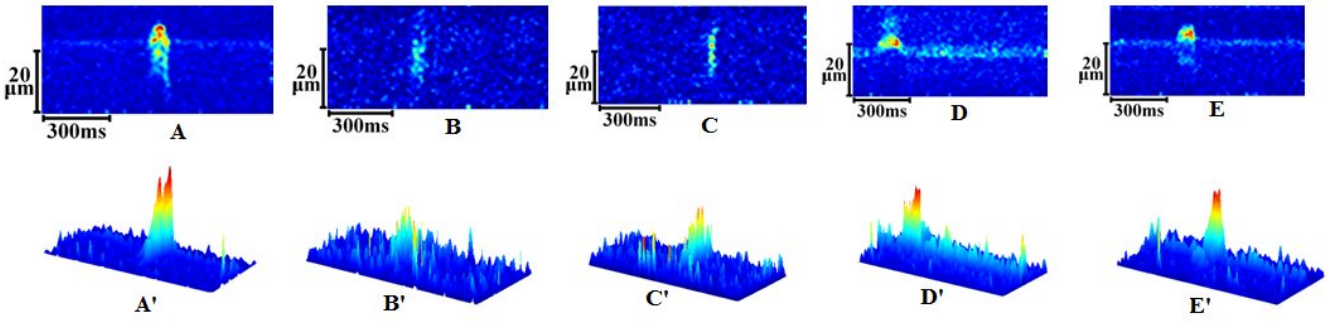

Figure 3. Representative confocal line-scan images of $I_{Ca.L}$-induced Ca^{2+} transients in sham operated group (A), HF (B), low dose (C), medium dose (D) and high dose (E) group. 3D images of $I_{Ca.L}$-induced Ca^{2+} transients in sham operated group (A'), HF (B'), low dose (C'), medium dose (D') and high dose (E') group.

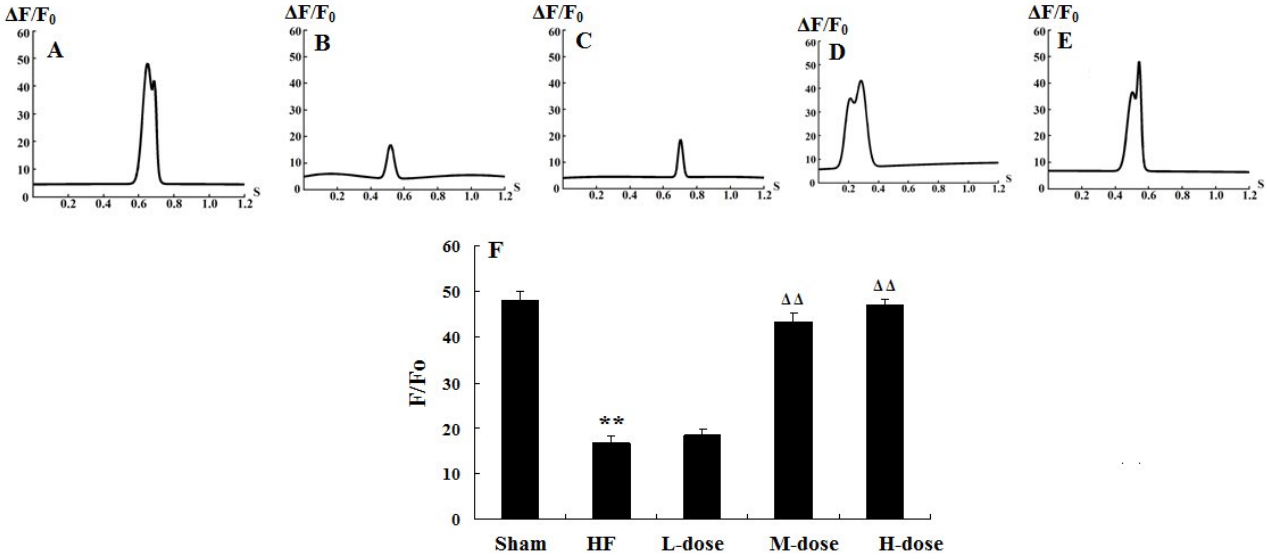

Figure 4. The spatial averages of $I_{Ca.L}$-induced Ca^{2+} transients in sham operated group (A), HF (B), low dose (C), medium dose (D) and high dose (E) group. The average amplitudes ($\Delta F/F_0$) of $I_{Ca.L}$-induced Ca^{2+} transients were 48.1±1.77in sham operated group, 16.7±1.29 in HF, 18.51±1.24 in low dose, 43.33±1.92 in medium dose and 47.21±1.25in high dose group (F). (P<0.01 versus sham group; $^{\Delta\Delta}P$<0.01 versus HF, n=10 cells from five sham operated group hearts, n=12 cells from six HF, low dose, medium dose and high dose group hearts, respectively)**

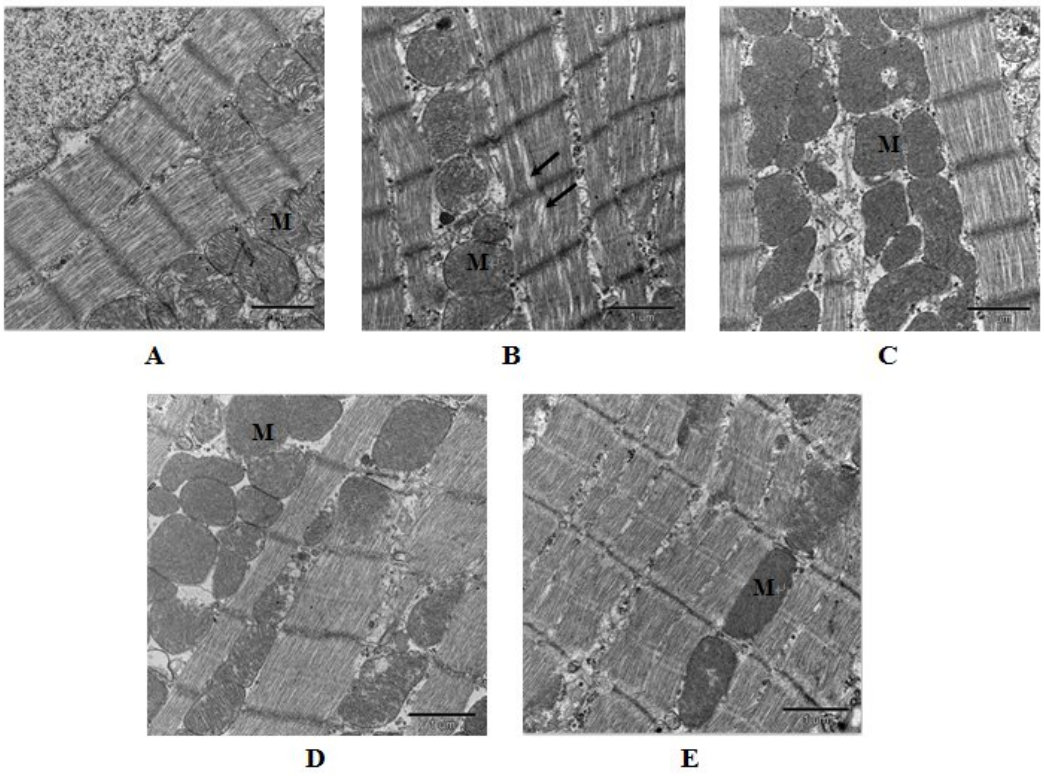

Figure 5. The ultrastructure of myocardial cells in different groups. In sham group (A), the myocardial cell appeared normal with intact sarcomeres, mitochondria (M) contain tightly packed cristae. Numerous glycogen granules were present. In HF group (B), some parts of the myocardial cell appeared intermyofibrillar lysis (arrows) and vesicles of varying size, mitochondria were swollen, and mitochondrial cristae were separated. In low dose group (C), intermyofibrillar lysis slightly restored, but a few mitochondria were still swollen, and mitochondrial cristae were separated. In medium dose group (D), intermyofibrillar lysis disappeared, myofilaments were orderly, closely, and evenly arranged, and mitochondria contain tightly packed cristae. The high dose group (E) was similar with that of middle dose group, and electron density of some mitochondria increased. (Magnification × 30,000)

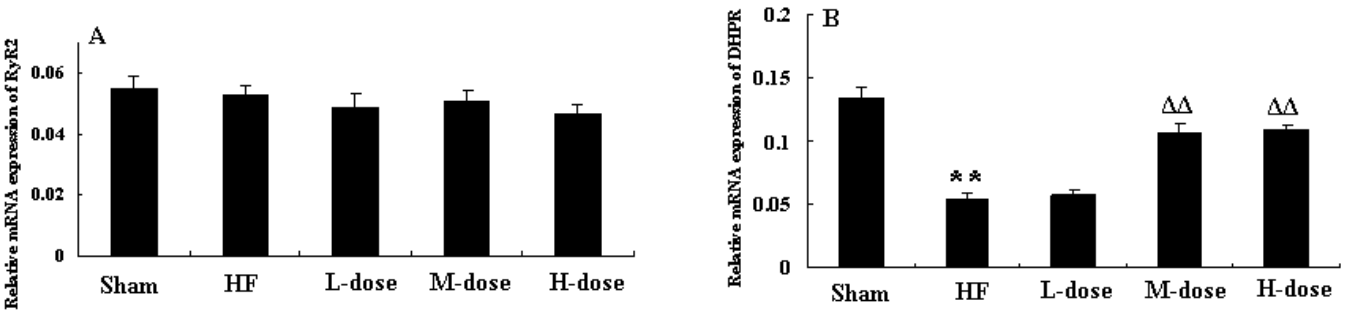

Fig.6. Relative expression of Ca^{2+} handling genes RyR2(A) and DHPR (B) in the different groups. (n = 8, **P<0.01 versus sham group; $^{\Delta\Delta}P$<0.01 versus HF)

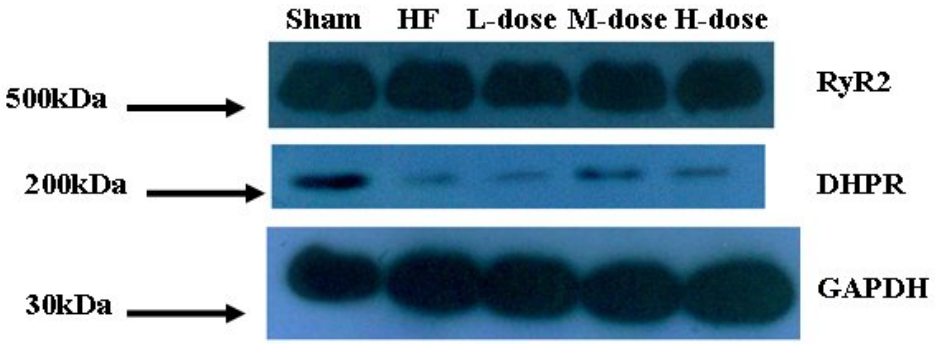

Figure 7. Expression of RyR2, DHPR and GAPDH in the sham, HF, low-dose, medium-dose and high-dose group. Arrows on the left indicate the position of molecular weight marker run in parallel to indicate protein migration on the gel.

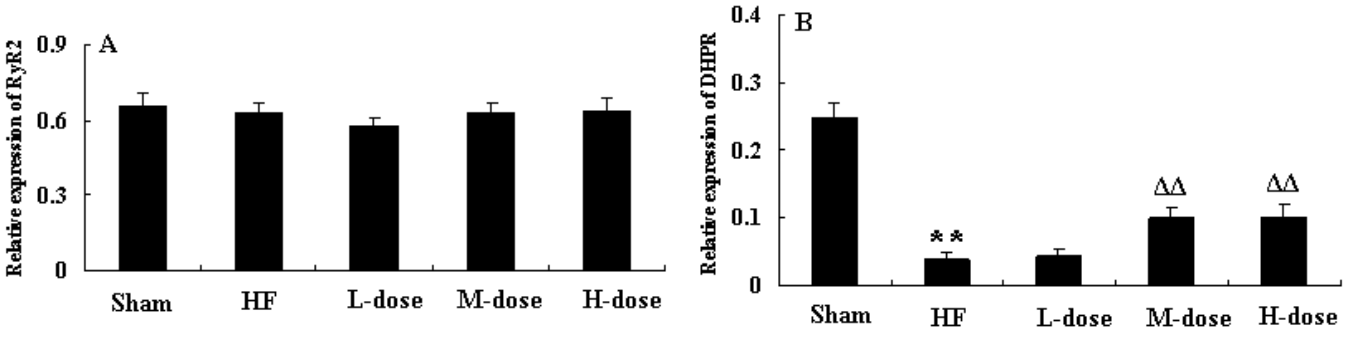

Figure 8. Relative amount of Ca^{2+} handling proteins RyR2 (A) and DHPR (B) in the different groups. (n = 6, **P<0.01 versus sham group; $^{\Delta\Delta}P$<0.01 versus HF)